Large-scale micromagnetic simulation of Nd-Fe-B sintered magnets with Dy-rich shell structures

Cite as: AIP Advances **6**, 056006 (2016); https://doi.org/10.1063/1.4943058
Submitted: 04 November 2015 • Accepted: 03 December 2015 • Published Online: 25 February 2016

T. Oikawa, H. Yokota, T. Ohkubo, et al.

Large-scale micromagnetic simulation of Nd-Fe-B sintered magnets with Dy-rich shell structures

T. Oikawa,[1,2] H. Yokota,[1,2] T. Ohkubo,[1,a] and K. Hono[1]
[1]*National Institute for Materials Science (NIMS), Tsukuba, 305-0047, Japan*
[2]*TDK Corporation, Ichikawa, 272-8558, Japan*

(Presented 12 January 2016; received 4 November 2015; accepted 3 December 2015; published online 25 February 2016)

Large-scale micromagnetic simulations have been performed using the energy minimization method on a model with structural features similar to those of Dy grain boundary diffusion (GBD)-processed sintered magnets. Coercivity increases as a linear function of the anisotropy field of the Dy-rich shell, which is independent of Dy composition in the core as long as the shell thickness is greater than about 15 nm. This result shows that the Dy contained in the initial sintered magnets prior to the GBD process is not essential for enhancing coercivity. Magnetization reversal patterns indicate that coercivity is strongly influenced by domain wall pinning at the grain boundary. This observation is found to be consistent with the one-dimensional pinning theory. [http://dx.doi.org/10.1063/1.4943058]

I. INTRODUCTION

Nd-Fe-B sintered magnets contribute to improving the performance of motors due to their high energy product. In recent years, applications of these magnets to traction motors for (hybrid) electric vehicles have been growing. For such applications, a room temperature coercivity of 3.0 T is required to avoid the demagnetization of the magnets during service at an elevated temperature. This room temperature coercivity can be achieved by the partial substitution of Dy for Nd in $Nd_2Fe_{14}B$, as the large magnetocrystalline anisotropy of $(Nd,Dy)_2Fe_{14}B$ contributes to coercivity enhancement. However, in $(Nd,Dy)_2Fe_{14}B$, the magnetic moment of Dy couples to that of Fe antiferromagnetically, which reduces the magnetization of Dy-substituted Nd-Fe-B magnets. In addition, Dy is one of the critical scarce elements to stable supply; therefore, its usage should be conserved. For these reasons, the content of Dy in (Nd,Dy)-Fe-B magnets must be reduced while maintaining high coercivity.

In Nd-Fe-B sintered magnets, magnetization reversal progresses by the penetration of reverse domains from grain boundaries (GBs) to the inside of crystal grains. Hence it is expected that Dy substitution only near GBs effectively enhances coercivity. This idea has been demonstrated with the grain boundary diffusion process (GBDP).[1] In GBDP, Dy is transferred from the sample surface to the interior of magnets mainly through GBs. It is known that the coercivity after GBDP does not exceed 2.0 T unless the initial sintered magnets are alloyed with Dy. Therefore in real products with coercivity of around 3.0 T, Dy is alloyed to the initial sample using the binary alloy method. The coercivity achievable through GBDP increases with the Dy concentration in the initial sintered magnets. Although this is a well-established experimental fact, it is not well-understood whether the Dy alloying in the initial sintered magnets is essential to achieve such high coercivity. In GBDP magnets, a Dy-rich shell is formed in the outer regions of the grains. The Dy-rich shell usually shows very distinct interfaces with the core region,[2,3] and the Dy concentration of the core is nearly the same as that of the initial sintered magnets.[2,3] Here a question arises: is the Dy alloying in

[a]Corresponding author: ohkubo.tadakatsu@nims.go.jp

the core region essential to achieve high coercivity in GBDP magnets? Or, alternatively, is the Dy concentration in the shell region the only factor responsible for coercivity enhancement? This study has been carried out to answer these questions.

In recent years, the relationship between the coercivity and the microstructure of sintered magnets, such as the grain size and the composition of the Nd-rich GB phase, has been experimentally clarified.[4,5] To interpret these experimental results, micromagnetic simulations for various model structures have been employed.[6,7] The modeled structures for the simulation must include multiple grains and thin GB layers, because the statistical treatment of the domain wall propagation through the GB layers is necessary to understand the magnetization reversal mechanism of sintered magnets. To simulate Nd-Fe-B magnets, a small mesh size of less than the exchange length of 1.7 nm is favorable for an accurate treatment of domain wall motion.[6] In order to satisfy both the requirements for a realistic microstructure and a small mesh size, the total number of finite elements can be more than 10 million, making large-scale parallel computation using a supercomputer necessary.[8,9] Recently, an energy minimization method was applied to Nd-Fe-B magnets, which accelerates the calculation speed by searching for the local minimum state of magnetic free energy quite efficiently.[10,11] In this study, the energy minimization method enables the simulation of a large model with 20 million elements within several hours of calculation time, as the calculation speed is accelerated by a factor of 20 compared to the conventional micromagnetic treatment. It is also reported that the energy minimization method is suitable for massive parallel computers such as the K computer because it exhibits high parallel calculation efficiency.[11]

In this paper, magnetization reversal processes are simulated for various (Nd,Dy)-Fe-B magnets with core-shell structures with different Dy concentrations in their shells and cores, using the energy minimization method. The aim is to answer the question of whether the alloying of $Nd_2Fe_{14}B$ with Dy is essential to achieve high coercivity through GBDP.

II. CALCULATION METHOD

A. Micromagnetics

The magnetization dynamics in micromagnetic simulations are described by Landau-Lifshitz-Gilbert (LLG) equation. The sweeping time of the external field for measuring M-H curves is of the order of a few seconds, which is significantly longer than the order of nano seconds treated to solve the LLG equation numerically. Therefore, in the time scale to discuss coercivity, the magnetization state can be approximated to be a local minimum state of the magnetic free energy at every point of the external field. In this situation the basic equation is represented as

$$\frac{\partial \boldsymbol{m}}{\partial \mathrm{t}} = -\boldsymbol{m} \times \left(\boldsymbol{m} \times \boldsymbol{H}_{eff}\right) \tag{1}$$

where $\boldsymbol{m}$ and $\boldsymbol{H}_{eff}$ are the normalized magnetization vector and effective field, respectively. The effective field is given by the following formula

$$\boldsymbol{H}_{eff} = \boldsymbol{H}_{ext} + \boldsymbol{H}_{ani} + \boldsymbol{H}_{exc} + \boldsymbol{H}_{d} \tag{2}$$

where $\boldsymbol{H}_{ext}$, $\boldsymbol{H}_{ani}$, $\boldsymbol{H}_{exc}$, and $\boldsymbol{H}_{d}$ are external field, anisotropy field, exchange coupling field, and demagnetization field, respectively. This basic equation corresponds to the LLG equation that neglects the precession term to enable efficient convergence to the local energy minimum state. The steepest decent method is applied to numerically solve the equation,[10,11] and the energy minimization code used in this study is based on Furuya *et al.*[11] The simulation is performed using a supercomputer (SGI ICE X) introduced in NIMS, and parallel calculations within 1728 cores are carried out.

B. Calculation model

The structure of the simulation model is shown in Fig. 1. In this model, each Nd-Fe-B grain has a core-shell structure and the grains are separated by a GB phase to simulate the structure

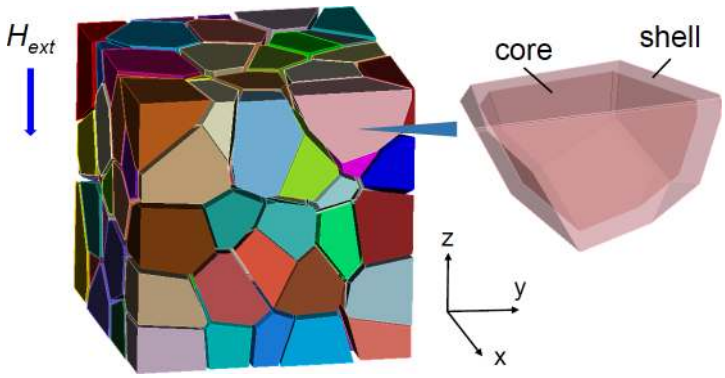

FIG. 1. Structure of the polycrystalline model created by the Voronoi tessellation of a cube. Each grain has a core-shell structure, in which a core is surrounded by a shell. The external field is applied in the z-direction (c-axis).

of GBD-processed Nd-Fe-B sintered magnets.[2,3] Polyhedral grains are created using the Voronoi tessellation of a cube. The model size is 300×300×300 nm^3 containing125 grains. The c-axis (the easy direction of the magnetization vector) is aligned to the z-direction and an external magnetic field is also applied in this direction. The GB phase is the space that is created by shrinking every grain with respect to its Voronoi generating point and subsequently subtracting all of them from the original cube. In the same manner, the shell is created as the space between the original and the shrunk polyhedral grain. The model consists of about 20 million tetrahedral elements, and a mesh size of 2.5 nm is applied since magnetization reversal patterns and coercivity are almost the same between 2.5 nm and 1.25 nm. The thicknesses of both the GB phase and the shell are set to 5 nm unless otherwise noted.

The material parameters of $Nd_2Fe_{14}B$ are taken from Ref. 12 by Sagawa *et al.*: the anisotropy constant $K_1 = 4.5$ MJ/m^3, the saturation magnetization $Js = 1.61$ T, and the exchange stiffness $A = 12.5$ pJ/m. The material parameters of $Dy_2Fe_{14}B$ are adopted from Ref. 13 by Hirosawa *et al.*: $K_1 = 4.2$ MJ/m^3, and $Js = 0.712$ T. Referring to these works, the parameters of $(Nd_{1-x}Dy_x)_2Fe_{14}B$ ($0 \leq x \leq 1$) are set as follows: K_1 and A are fixed to the value of $Nd_2Fe_{14}B$, and Js is interpolated linearly to x from the $Nd_2Fe_{14}B$ to $Dy_2Fe_{14}B$ value. The anisotropy field H_A is defined as $H_A = 2K_1/J_S$, but it is a substantially linear function of x for narrow region ($0 \leq x \leq 0.3$). The GB phase is set to be an amorphous soft magnet layer with material parameters: $K_1 = 0$, $J_S = 0.5$ T, and $A = 6$ pJ/m. Therefore, grains of the main phase are exchange coupled through the GB phase.

III. CALCULATION RESULTS AND DISCUSSIONS

Magnetization reversal is simulated for the model with a Dy-rich shell whose composition is described as $(Nd_{1-x}Dy_x)_2Fe_{14}B$ using a Dy substitutional rate x. The K_1 value of a selected grain located at the edge of the model surface is set to 1/10 of $Nd_2Fe_{14}B$, where a reverse domain nucleates and acts as a source of domain wall propagation. In real magnets, magnetization reversal occurs from the defects at the surface; hence, the present defect model is considered to simulate magnetization reversal processes in actual sintered magnets. Calculated demagnetization curves for a $Nd_2Fe_{14}B$ core is shown in Fig. 2(a). The curves are rectangular shaped and the coercivity increases with the Dy content of the shell region. Fig. 2(b) shows coercivity as a function of the H_A value of the shell, where the core compositions are (i) $Nd_2Fe_{14}B$, (ii) $(Nd_{1-x}Dy_x)_2Fe_{14}B$, and (iii) $(Nd_{1-x/2}Dy_{x/2})_2Fe_{14}B$ with the shell composition $(Nd_{1-x}Dy_x)_2Fe_{14}B$. The coercivity is a linear function of the H_A value of the shell and the increment from $x = 0$ exhibits an enhancement due to Dy substitution. The coercivity enhancement becomes slightly larger with increasing Dy content in the core; the enhancement shown in line (i) is about 90 % of line (ii). Fig. 3 shows the shell thickness dependence of the enhanced coercivity, where the shell composition is $x = 0.3$, and the core composition is $Nd_2Fe_{14}B$. The dotted line shows the enhanced coercivity when the core composition is also $x = 0.3$, which corresponds to the limit of a very thick shell. In fact, the coercivity is further

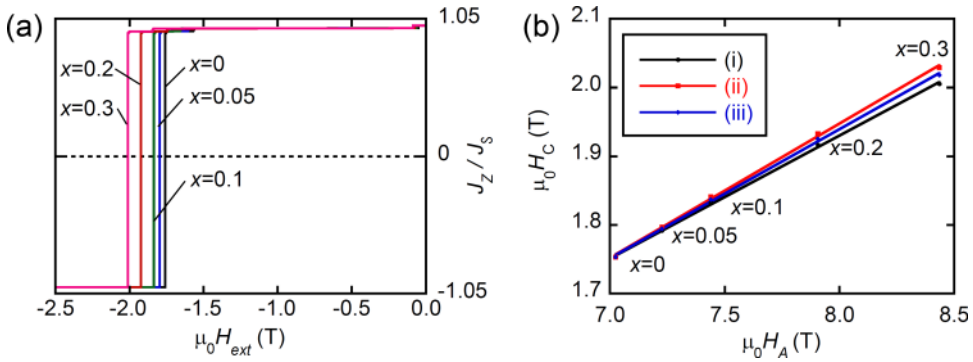

FIG. 2. (a) Demagnetization curves for various Dy content x within the shell, where the core contains no Dy. (b) The relationship between the coercivity and the anisotropic field of the shell. The Dy composition of the core is 0 in (i), x in (ii), and $x/2$ in (iii).

enhanced with increasing shell thickness, and saturates at about 15 nm. This result indicates that almost all of the contribution of the coercivity increment can be attributed to the H_A value of the shell if the shell thickness is greater than about 15 nm. As mentioned above, even if the shell thickness is 5 nm, 90 % of the coercivity enhancement that can be expected from a fully Dy-substituted alloy can be obtained. Hence, we can conclude that Dy alloying in the initial sintered magnets prior to GBDP is not essential. Generally, GBDP is carried out at around 900°C, and the Dy concentration in the shell is limited by the thermodynamic equilibrium between the core-$(Nd,Dy)_2Fe_{14}B$ and the (Nd,Dy)-rich liquid phases.[3] As a consequence, the Dy concentration in the shell cannot reach the level that is required to achieve 3.0 T of coercivity unless Dy is alloyed in the core. Sepehri-Amin *et al.* applied GBDP to hot-deformed Nd-Fe-B magnets at 650°C using a $Nd_{60}Dy_{20}Cu_{20}$ eutectic alloy, and they could increase the shell Dy composition x up to 0.4.[14] In a similar manner, if a low processing temperature could be applied to the GBDP of sintered magnets, a high Dy concentration in the shell structure is expected.

Fig. 4 shows the magnetization reversal patterns of (Nd,Dy)-Fe-B magnets with surface views (Fig. 4(a)) and cross-sectional views (Fig. 4(b)). The viewing direction of Fig. 4(a) is the same as that of Fig. 1. The Dy composition of the shell is $x = 0$ and $x = 0.3$, and that of the core is $x = 0$. The initial magnetization state (in the +z direction) is shown in red, and the reversed state (in the -z direction) is shown in blue. The magnetization states are represented by the normalized magnetization m_z defined as J_Z/J_S. At the beginning of the reversal processes, the reverse domain

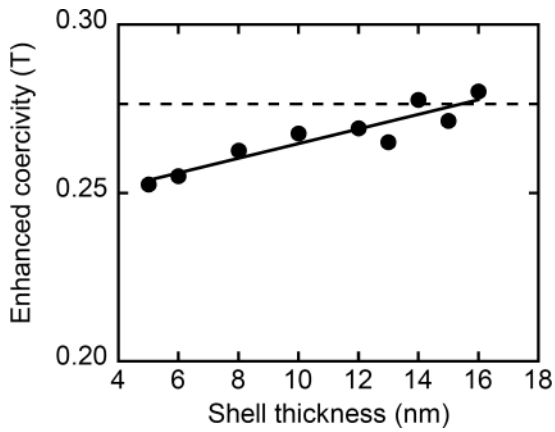

FIG. 3. Coercivity enhancement by varying the thickness of the shell. The Dy composition of the shell is $x = 0.3$, and the core contains no Dy. The dotted line shows the enhanced coercivity when the core composition is the same as the shell composition.

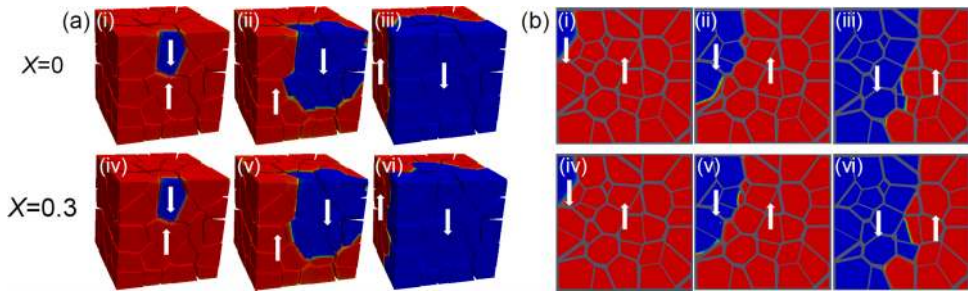

FIG. 4. Magnetization reversal patterns of (Nd,Dy)-Fe-B magnets in (a) the surface view, and (b) the cross-sectional view (in the y=0 plane). The Dy composition of the shell is x=0 and 0.3, and the core contains no Dy. The normalized magnetization m_z is as follows; (i)m_z = 0.98, (ii)m_z = 0.64, (iii)m_z = -0.06, (iv)m_z =0.98, (v)m_z = 0.65, and (vi)m_z = -0.03 .

nucleates in the introduced defected grain with a small value of K_1. From this site the reverse domain expands along the c-axis direction due to the magnetostatic field. After reaching the bottom surface, it expands in the transverse direction. This domain expansion feature is more clearly observed in Fig. 4(b). It is also revealed that the magnetization reversal features are almost the same between $x = 0$ and $x = 0.3$ for the same m_z values, although the applied magnetic field is different.

The above magnetization reversal patterns indicate that the main process for determining coercivity is the pinning of the reverse domains at GBs, and the anisotropy field of the shell influences the domain wall pinning strength. No pinning force may act within cores because of the uniformity of the magnetic properties. In the three-dimensional (3-D) polycrystalline model, the pinning mechanism is so complicated that the enhanced coercivity is discussed using a one-dimensional (1-D) planer model.[15,16] Scholz *et al*. investigated the potential barrier thickness dependence of the pinning field (H_{pin}) using 1-D micromagnetic simulations.[17] They demonstrated that H_{pin} increases with increasing barrier thickness and saturates at around the domain wall width. As can be seen in Fig. 2(b), the coercivity reaches 99 % of its saturation when the shell thickness is 5 nm (the estimated domain wall width is 5.2 nm). Thus, our result is consistent with the results of Scholz *et al*. because the shell structure can be taken as the potential barrier to a domain wall. As a result, the coercivity enhancement resulting from a Dy-rich shell can be qualitatively explained using the 1-D pinning model. Although GBs consist of connected polyhedral surfaces, local pinning processes may be similar to those of a simple planar surface. When the grain size increases, the coercivity mechanism might be modified because the stray field of defect grains increases and comparatively strengthens the contribution of magnetostatic coupling among grains.

IV. CONCLUSION

Magnetization reversal of (Nd,Dy)-Fe-B magnets was simulated using an energy minimization method. The model includes core-shell structured grains and a thin GB layer as the microstructure of GBD processed magnets. Enhanced coercivity is a linear function of the anisotropy field of the shell, and it turns out to be independent of the Dy composition of the core if the shell thickness is greater than about 15 nm. Therefore, Dy alloying in the initial sintered magnets is not essential if the Dy concentration in the shell can be increased to the necessary level to achieve a value of H_A for higher coercivity (3.0 T). If the Dy composition of the shell alone can be increased by some novel low-temperature process, it is expected that Dy-free Nd-Fe-B alloys can be used as initial sintered magnets, which introduces the significant benefit of conserving Dy as a critical scarce element as well as increasing the remanent magnetization. Magnetization reversal patterns are independent of the shell and core Dy compositions, and domain wall pinning at the GB is shown to be the principle origin of coercivity. Coercivity is almost constant when the shell thickness is larger than the domain wall width, and this can be explained using 1-D pinning theory.

[1] K. Hirota, H. Nakamura, T. Minowa, and M. Honshima, IEEE Trans. Mag. **42**, 2909 (2006).
[2] H. Sepehri-Amin, T. Ohkubo, and K. Hono, Acta Mater. **61**, 1982 (2013).
[3] U. M. R. Seelam, T. Ohkubo, T. Abe, S. Horosawa, and K. Hono, J. Alloys Comp. **617**, 884 (2014).

[4] K. Hono and H. Sepehri-Amin, Scripta Mater. **67**, 530 (2012).
[5] H. Sepehri-Amin, T. Ohkubo, T. Shima, and K. Hono, Acta Mater. **60**, 819 (2012).
[6] D. Süss, T. Schrefl, and J. Fidler, IEEE Trans. Mag. **36**, 3282 (2000).
[7] T. Schrefl, T. Shoji, M. Winklhofer, H. Oezelt, M. Yano, and G. Zimanyi, J. Appl. Phys. **111**, 07A728 (2012).
[8] J. Fujisaki, A. Furuya, Y. Uehara, K. Shimizu, H. Oshima, T. Ohkubo, S. Hirosawa, and K. Hono, IEEE Trans. Mag. **50**, 7100704 (2014).
[9] N. Inami, Y. Takeichi, C. Mitsumata, K. Iwano, T. Ishikawa, S. –J. Lee, H. Yanagihara, E. Kita, and K. Ono, IEEE Trans. Mag. **50**, 1400304 (2014).
[10] L. Exl, S. Bance, F. Reichel, T. Schrefl, H. P. Stimming, and N. J. Mauser, J. Appl. Phys. **115**, 17D118 (2014).
[11] A. Furuya, J. Fujisaki, K. Shimizu, Y. Uehara, T. Ataka, T. Tanaka, and H. Oshima, IEEE Trans. Mag. **51**, 2103004 (2015).
[12] M. Sagawa, S. Fujimura, H. Yamamoto, Y. Matsuura, and S. Hirosawa, J. Appl. Phys. **57**, 4094 (1985).
[13] S. Hirosawa, Y. Matsuura, H. Yamamoto, S. Fujimura, M. Sagawa, and H. Yamauchi, J. Appl. Phys. **59**, 873 (1986).
[14] H. Sepehri-Amin, J. Liu, T. Ohkubo, K. Hioki, A. Hattori, and K. Hono, Scripta Mater. **69**, 647 (2013).
[15] J. Fidler, T. Schrefl, W. Scholz, D. Suess, R. Dittrich, and M. Kirschner, J. Magn. Magn. Mater. **272-276**, 641 (2004).
[16] H. Kronmüller and D. Goll, Physica B **319**, 122 (2002).
[17] W. Scholz, T. Schrefl, J. Fidler, T. Matthias, D. Suess, and V. Tsiantos, IEEE Trans. Mag. **2920** (2003).